AD NUMBER

AD467419

LIMITATION CHANGES

TO:

Approved for public release; distribution is unlimited.

FROM:

**Distribution authorized to U.S. Gov't. agencies and their contractors;
Administrative/Operational Use; MAY 1965. Other requests shall be referred to Defense Advanced Research Projects Agency, 675 North Randolph Street, Arlington, VA 22203-2114.**

AUTHORITY

ONR ltr, 28 Jul 1977

SU-SEL-65-062

HF Radio Measurements of the High-Altitude Acoustic Effects of a Ground-Level Explosion

by
L. J. Griffiths
G. H. Barry
J. C. Taenzer

May 1965

Technical Report No. 107

Prepared under
Office of Naval Research Contract
Nonr-225(64), NR 088 019, and
Advanced Research Projects Agency ARPA Order 196-65

RADIOSCIENCE LABORATORY

STANFORD ELECTRONICS LABORATORIES

STANFORD UNIVERSITY • STANFORD, CALIFORNIA

SEL-65-062

HF RADIO MEASUREMENTS OF THE HIGH-ALTITUDE ACOUSTIC EFFECTS OF A GROUND-LEVEL EXPLOSION

by

L. J. Griffiths
G. H. Barry
J. C. Taenzer

May 1965

Technical Report No. 107

Prepared under
Office of Naval Research Contract
Nonr-225(64), NR 088-019, and
Advanced Research Projects Agency ARPA Order 196-65

Radioscience Laboratory
Stanford Electronics Laboratories
Stanford University Stanford, California

ABSTRACT

An hf radio experiment was performed to measure the high-altitude effect of the vertically traveling pressure wave resulting from a large ground-level explosion. The blast--Project Snowball--consisted of 500 tons of TNT and was detonated at the Suffield Experimental Station, Alberta, Canada, July, 1964. The ionospheric disturbance was monitored using vertical-incidence, phase-sensitive sounders located 85 km from ground zero.

Simple, linear, acoustic theory was used to calculate the onset time, amplitude, and period of the radio-signal disturbance. These calculations agree closely with measurements taken by the vertical-incidence sounders--onset time was predicted within 10 sec, and both amplitude and period agreed within a factor of two.

CONTENTS

TABLE

ILLUSTRATIONS

ILLUSTRATIONS (Cont)

ACKNOWLEDGMENT

The authors wish to thank Mr. David M. Annett for his extensive efforts in directing the experimental portion of this study.

We are also grateful for the helpful assistance of Mr. Charles N. Kingery of D.A.S.A. Headquarters, Mr. Fred Davey of the Field Experimental Site at the Suffield Experimental Station, and Mr. James Holdsworth of the Canadian Defence Research Northern Laboratories.

I. INTRODUCTION

On 17 July 1964, at 1058 MST, approximately 500 tons of TNT was detonated on the ground surface at the Suffield Experimental Station (SES), Ralston, Alberta, Canada (Fig. 1). The detonation culminated a comprehensive program of blast studies, under the sponsorship of the Canadian Defence Research Board, under a tripartite arrangement with Canada, the United Kingdom, and the United States represented. The U. S. participation in this test was named Operation Snowball. Stanford's primary objective in participating in this program was to study the effect of the blast on the ionosphere.

The shock wave initially generated by the atmospheric explosion degenerates rapidly into a low-frequency sound wave, which then

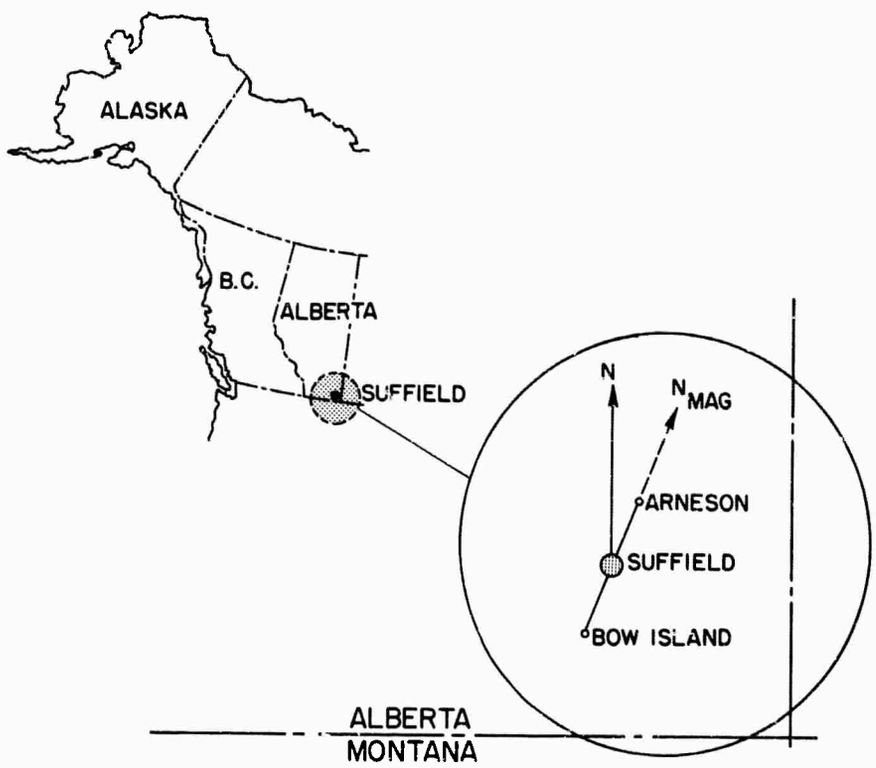

32301

FIG. 1. LOCATION OF SNOWBALL EXPLOSION.

propagates to great distances with little attenuation. Acoustic energy directed vertically, for example, can reach the ionized regions of the extreme upper atmosphere. The effect of such pressure disturbance on the ionosphere may be studied from the ground using high-frequency (hf) radio signals that reflect vertically from the ionized layer directly above the blast (Fig. 2). The disturbance causes localized electron-density variations, which, in turn, influence the phase path of the reflecting radio wave.

For the purpose of instrumenting the ionosphere above the Snowball explosion, two vertical-incidence, phase-sensitive ionospheric sounders were located 50 miles magnetic north and south of the blast--near the towns of Arneson and Bow Island (Fig. 1)-- in an attempt to measure the influence of the earth's magnetic field on acoustic-wave propagation.

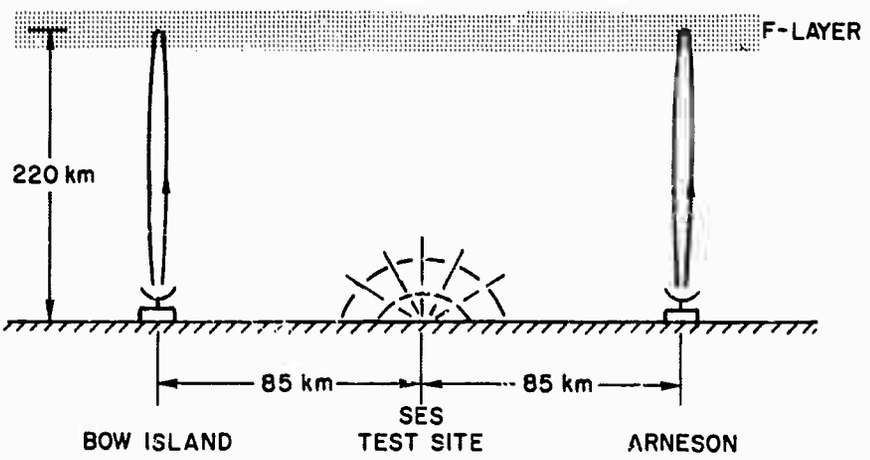

34267

FIG. 2. CROSS SECTION SHOWING EXPLOSION AND GEOMETRY OF VERTICAL-INCIDENCE PULSE SOUNDER.

II. THEORY

The following section presents a brief outline of the method used to predict the disturbance detected by ionospheric sounders operating near the 500-ton Snowball explosion. The theory is presented in two parts: a calculation of the size and shape of the pressure wave produced in the ionosphere by the blast, and a prediction of the effect of such a pressure disturbance on an hf radio-wave reflection from the ionosphere.

A. PROPAGATION OF EXPLOSION-INDUCED SHOCK WAVES

The mathematical description of the propagation of acoustic waves generated by explosions in the atmosphere is facilitated by considering separately near- and far-field effects. The shock wave traveling in the near field must be described by a set of nonlinear differential equations. For the purposes of this paper, the blast-wave computations of Brode [Ref. 1] were used to describe near-field effects. Brode's results extend from the surface of the explosive out to a point at which the maximum shock overpressure has been reduced to 6 percent. Figure 3 shows the 6-percent wave shape given for a 500-ton blast.

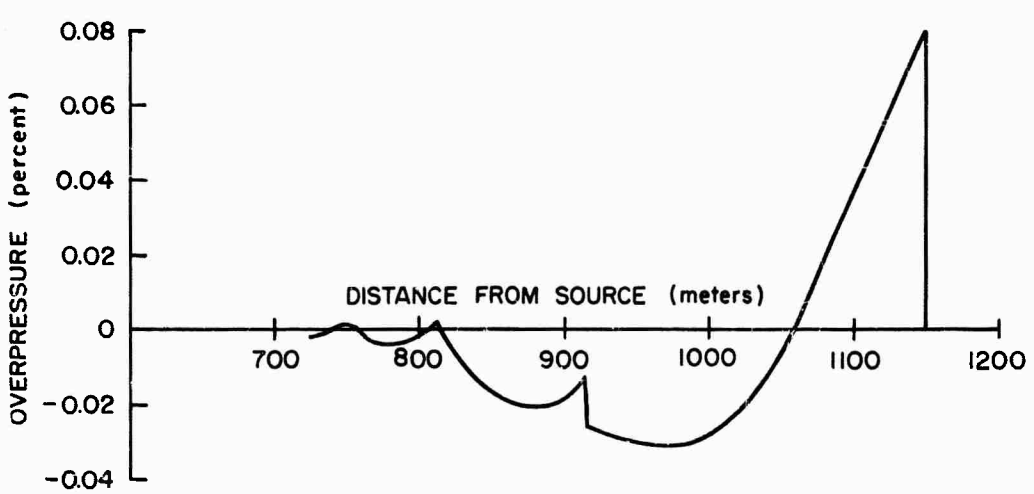

34268

FIG. 3. PRESSURE VS DISTANCE FROM SOURCE FOR SHOCK WAVE AT 6-PERCENT OVERPRESSURE.

From this point outward, the disturbance may be treated as a linear acoustic wave. To simplify calculations, an approximation to Brode's waveform (Fig. 4) was assumed uniformly distributed over a hemispherical wavefront 1150 meters from the source (Fig. 5). The following discussion summarizes the linear acoustic theory used to describe propagation in the far-field regions.

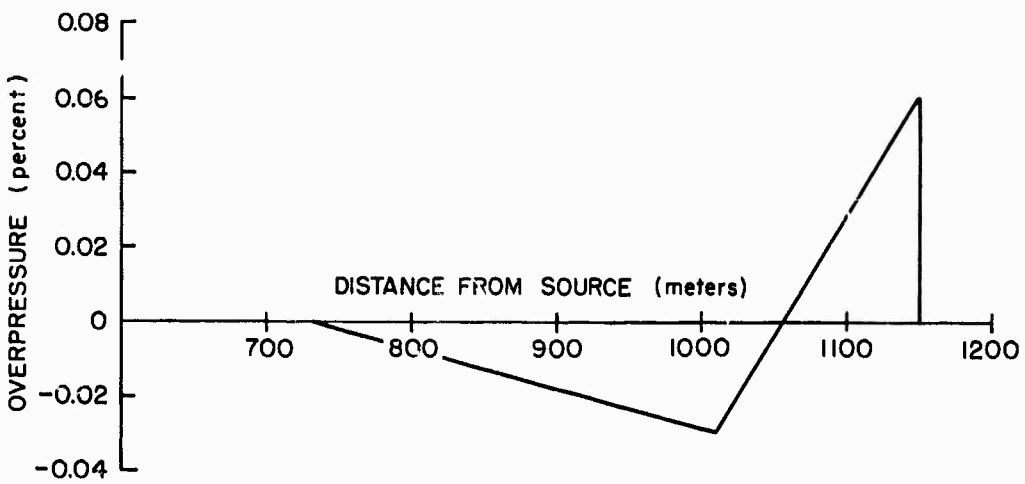

34269

FIG. 4. STRAIGHT-LINE APPROXIMATION OF 6-PERCENT OVERPRESSURE USED IN CALCULATIONS OF THIS REPORT.

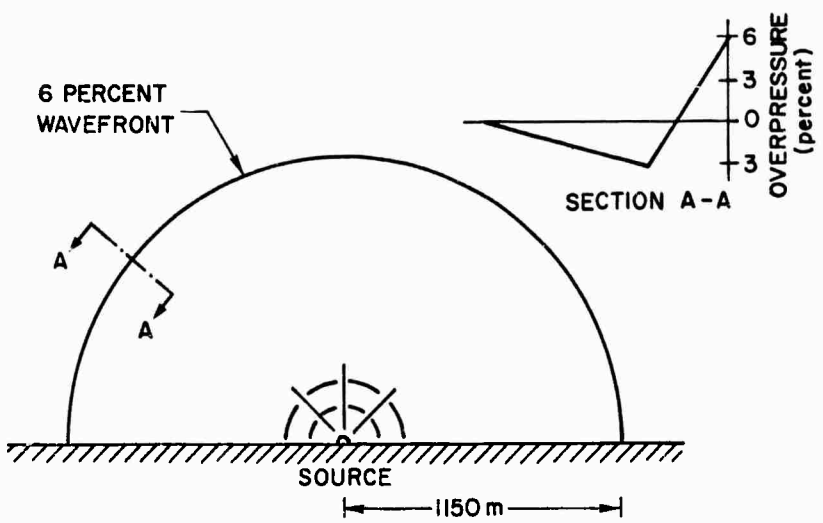

34270

FIG. 5. 6-PERCENT WAVEFRONT USED IN CALCULATIONS OF THIS REPORT

The maximum power density carried by a linear, plane, harmonic acoustic wave in the atmosphere is given by the equation [Ref. 2]

$$P = \frac{\rho a^3}{2\gamma^2}\left(\frac{p_{max} - p_o}{p_o}\right)^2 , \qquad (1)$$

where ρ = atmospheric density

a = velocity of sound

γ = ratio of specific heats, C_p/C_v

p_{max} = maximum pressure in the wave

p_o = ambient atmospheric pressure.

One may relate the acoustic properties of a wave propagating from point 1 to point 2 in the atmosphere in terms of the properties at each point by the simple ratio

$$\left(\frac{\pi_2}{\pi_1}\right)^2 = \left(\frac{\gamma_2}{\gamma_1}\right)^2 \left(\frac{\rho_1}{\rho_2}\right)\left(\frac{a_1}{a_2}\right)^3 \frac{P_2}{P_1} , \qquad (2)$$

where π is the peak normalized overpressure, $(P_{max} - p_o)/p_o$.

This equation is the basis of the linear acoustic theory used in this paper. The wave at point 1 is taken as the 6-percent wavefront and associated wave shape described by Brode. The wave properties at point 2--the ionosphere directly above the blast--are then calculated by using Eq. (2). Inspection of the equation shows immediately that all terms are defined except the maximum power-density ratio, P_2/P_1. (The values of ρ, a, and γ have been taken from U. S. Standard Atmosphere [Ref. 3].)

As a shock wave propagates upward in the atmosphere, the power density in the wave will be decreased by two separate mechanisms, each of which may be considered independently. The first loss is caused by spreading. Since the wavefront area becomes increasingly large with propagation away from the source, the total energy in the wave is spread over a larger area and both energy density and power density are reduced.

The second loss is introduced by atmospheric attenuation; in fact, the atmosphere acts as a lossy bandpass filter to sound waves.

Taking these effects into account, the power loss may be expressed as

$$\frac{P_2}{P_1} = \Delta P_s \, \Delta P_f \ , \qquad (3)$$

where ΔP_s = power-density loss factor caused by spreading

ΔP_f = power-density loss factor caused by atmospheric filtering.

Shock waves generated by explosions in a uniform atmosphere are spherical and remain spherical as the shock propagates outward; the power density is inversely proportional to the area of the front. Thus, the spreading loss factor ΔP_s (Eq. 3), for a disturbance propagating from the Brode 6-percent radius (i.e., 1150 meters from the source) to the upper ionosphere (i.e., F-layer at 220-km altitude) in a homogeneous atmosphere is $\Delta P_s = (1.15/220)^2 = 5.23 \times 10^{-6}$.

For the real atmosphere, the increased loss caused by nonuniform spreading was estimated with the use of acoustic raytracing (Fig. 6) and found to be about 0.3 times the value given for a homogeneous atmosphere. Thus

$$\Delta P_s = 1.57 \times 10^{-6} \ .$$

The atmospheric-filtering loss factor ΔP_f (Eq. 3) is obtained from the general wave equation for linear, plane acoustic waves.

$$\frac{p-p_o}{p_o}(x,t) = \frac{p_{max}-p_o}{p_o} \exp[-\alpha x] \exp\left[j2\pi f\left\{t-(x/a)\right\}\right] \qquad (5)$$

where α = attenuation constant (nepers/meter)

f = acoustic frequency

a = speed of sound

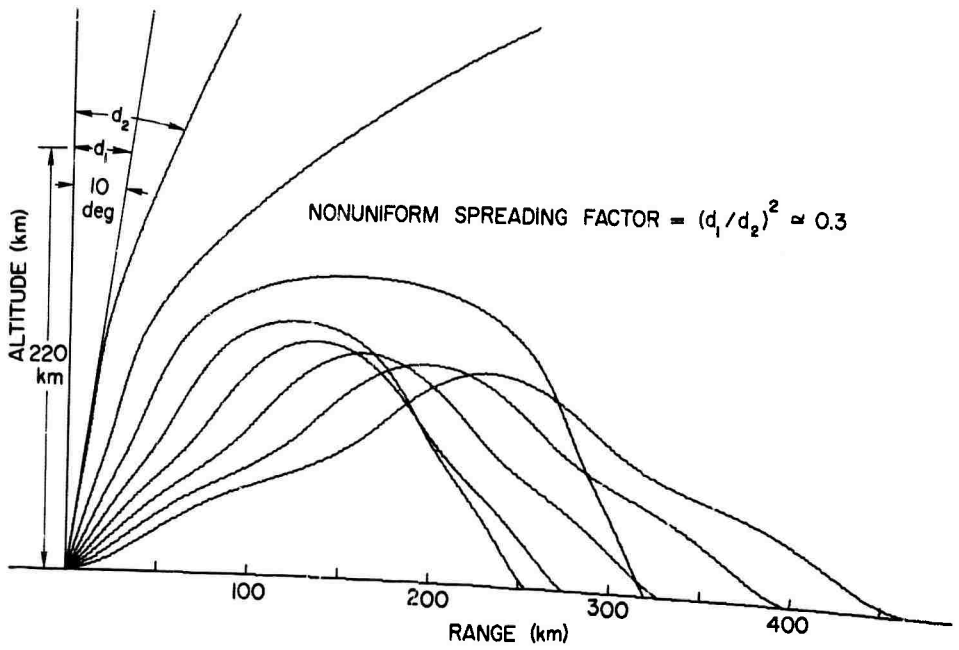

34271

FIG. 6. ACOUSTIC RAYTRACING FOR GROUND-LEVEL EXPLOSION--RAYS AT 10-DEG INCREMENTS.

The total power attenuation (in db) as a function of frequency for a wave traveling between two points x_1 and x_2 is then

$$\Delta P(f) = 8.68 \int_{x_1}^{x_2} \alpha(f,h)\, dx \quad db \quad . \tag{6}$$

The attenuation constant α is a function of frequency and altitude and was shown by Rayleigh [Ref. 2] to be

$$\alpha(f,h) = \frac{4\pi^2 f^2}{a^3} \left(\frac{4\eta}{3} + \frac{\gamma - 1}{\gamma} k \right) , \tag{7}$$

where η = kinematic viscosity

k = thermal conductivity

γ = ratio of specific heats, C_p/C_v .

Ignoring the generally much-smaller conductivity term and substituting [Ref. 2]

$$\eta = 0.499 \frac{v^2}{\nu} = \frac{1.497\ a^2}{\gamma \nu} ,$$

where v = mean particle velocity

ν = viscosity coefficient,

yields

$$\alpha(f,h) = \frac{2}{\gamma} \frac{4\pi^2 f^2}{\nu a} . \tag{8}$$

Substituting this value in Eq. (6) gives

$$\Delta P(f) = 3.42 \times 10^2 \int_{x_1}^{x_2} \frac{dx}{\nu a} \tag{9}$$

or

$$\Delta P(f) = K_{1-2}\ f^2 , \tag{10}$$

where

$$K_{1-2} = 3.42 \times 10^2 \int_{x_1}^{x_2} \frac{dx}{\nu a} . \tag{11}$$

The value of K_{1-2} was evaluated graphically with the point x_1 taken as the top of the 6-percent wavefront 1150 meters above the source and x_2 as the F layer at 220-km altitude. The resulting value was

$$K_{1-2} = 6.01 \times 10^3\ \text{sec}^{-2} .$$

Equation (9) above describes the attenuation of high acoustic frequencies. Propagation of low frequencies is limited by the cutoff frequency f_{co}, which is caused by the variation in atmospheric density

with altitude. The value of the lower limit may be obtained by observing that, to a vertically traveling sound wave, the atmosphere has the appearance of an exponentially tapered transmission line. The acoustic impedance is [Ref. 2]

$$z = a\rho \ , \tag{12}$$

where a is the velocity of sound and ρ is the atmospheric density. Although both the speed of sound and density vary with altitude, variations in the latter are much more pronounced, being approximately exponential. Thus,

$$\begin{aligned} \rho &= \rho_o \exp[-(h-h_o)/H] \\ &= \rho_o \exp[h_o/H] \exp[-h/H] \\ &= \rho_1 \exp[-h/H] \ , \end{aligned} \tag{13}$$

where h = altitude

H = scale height

ρ_o = density at some altitude h_o.

Substituting this in Eq. (12) gives

$$Z = a\rho_1 \exp[-h/H] \ . \tag{14}$$

The cutoff frequency for an exponentially tapered transmission line [Ref. 4] is

$$f_{co} = \frac{a}{4\pi H} \ . \tag{15}$$

Since both the velocity of sound and the scale height vary with height in a similar manner, the lowest useful frequency is not strongly height dependent. An average value of 0.004 cps, taken from Eq. (15) and atmospheric characteristics given in U. S. Standard Atmosphere [Ref. 3], was selected for use in this paper. Figure 7 summarizes the atmospheric-attenuation characteristics for a sound wave traveling vertically from ground level to 220-km altitude.

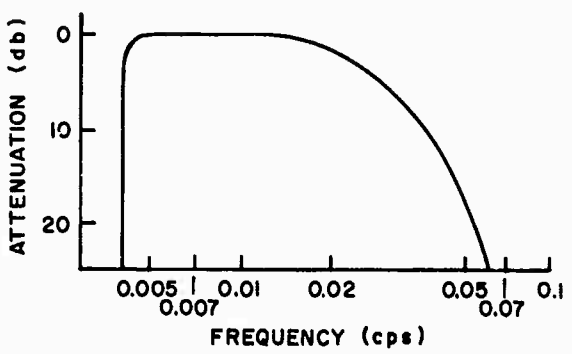

34272

FIG. 7. ATTENUATION AS A FUNCTION OF FREQUENCY.

The effect of atmospheric filtering on the particular acoustic wave f interest--i.e., Brode's 6-percent waveform--was determined by analog means. An electrical filter having the attenuation characteristics of Fig. 7 was constructed. When excited by a voltage wave shape identical to that of the Brode shock wave for 6-percent overpressure, the output signal represents the neutral acoustic disturbance in the F layer directly above the blast. The total acoustic-power loss factor caused by atmospheric filtering--i.e., ΔP_f of Eq. (1)--is the ratio of maximum-output to maximum-input voltage (Fig. 8).

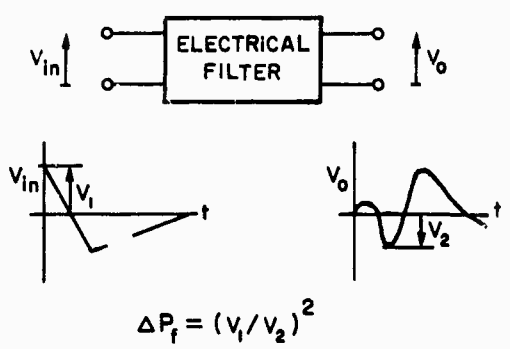

34273

FIG. 8. ANALOG TECHNIQUE USED TO DETERMINE POWER LOSS DUE TO SPECTRAL FILTERING.

The value of power-density loss factor obtained in this manner was

$$\Delta P_f = 4.75 \times 10^{-3} \quad . \tag{16}$$

Thus, when the values from Eqs. (4) and (16) are substituted into Eq. (3), the power-density ratio is

$$\begin{aligned} \frac{P_2}{P_1} &= \Delta P_s \times \Delta P_f \\ &= 1.57 \times 10^{-6} \times 4.75 \times 10^{-3} \\ &= 7.45 \times 10^{-9} \quad . \end{aligned}$$

The value of F-layer overpressure may now be determined from Eq. (2) with $\pi_1 = 6$ percent and the appropriate values of γ, ρ, and a taken from U. S. Standard Atmosphere. The predicted maximum F-layer overpressure is then found to be

$$\pi_2 = 2.2 \text{ percent.}$$

The above calculation has ignored the effect of ground reflections. For the case of perfect reflection, twice as much energy as considered above would be directed upward. Since overpressure is proportional to the square root of energy density--Eq. (1)--this effect could increase the predicted F-layer overpressure to a value

$$\pi_2 = 3.1 \text{ percent.}$$

The magnitude and wave shape of the predicted ionospheric pressure disturbance are shown in Fig. 9.

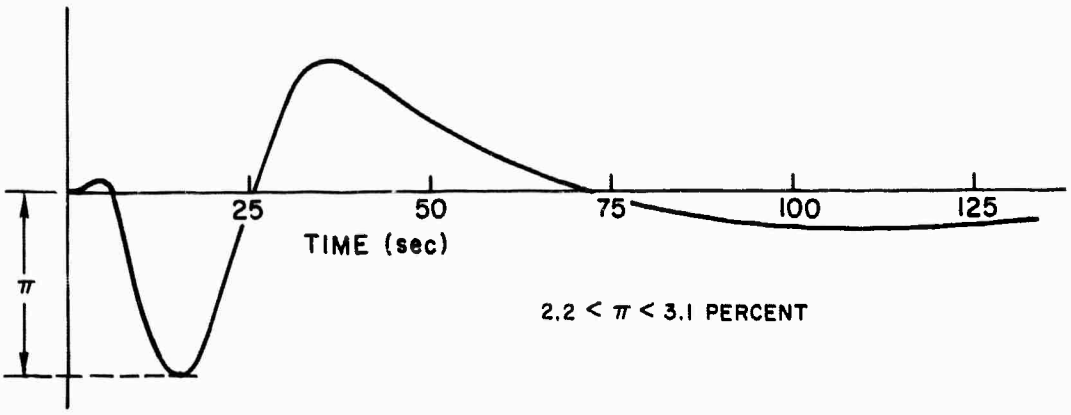

FIG. 9. OVERPRESSURE WAVEFORM AT 220 KM DETERMINED FROM ANALOG MODEL.

B. INTERACTION BETWEEN ACOUSTIC AND RADIO WAVES

Acoustic waves traveling in the lower ionosphere may be detected by phase measurements on hf radio signals reflected within the disturbed region. Neutral-density variations associated with an acoustic disturbance result in corresponding changes in electron density.* The radio-wave index of refraction μ is, of course, a function of the local electron density [Ref. 5]; the phase path of the radio signal is thus sensitive to any neutral pressure changes. The rate of phase change is the frequency shift or "modulation" observed at the radio receiver.

An hf radio wave vertically incident on the ionosphere splits into its ordinary (O) and extraordinary (X) components (Fig. 10) as a consequence of the geomagnetic field. The raypaths taken by the components depend on the frequency used, the magnetic-field geometry, and the structure of the ionosphere. Generally, for dip angles greater than 45 deg, the X wave deviates less from the normal than does the O wave.

Both components are sensitive to ionospheric fluctuations at any point along their paths. The greatest sensitivity, however, occurs

*In the absence of the geomagnetic field, or for acoustic waves traveling in a direction along the magnetic-field lines.

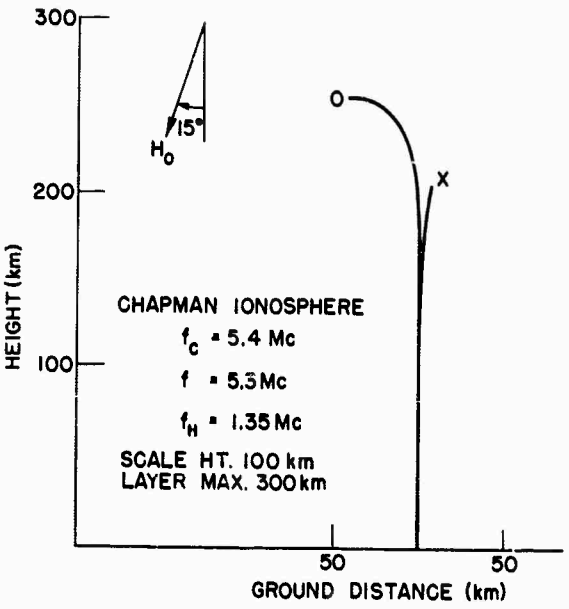

31556

FIG. 10. ORDINARY-EXTRAORDINARY RADIO-WAVE SPLITTING AT VERTICAL INCIDENCE.

near the point of reflection. It is clear, therefore, that the exact phase disturbance resulting from an acoustic wave propagating through the ionosphere is a function of a great number of variables.

For the purpose of calculation, several assumptions were used to simplify the problem. Only the X component was considered, and ray bending was ignored (Fig. 11). The ray was assumed to be perpendicularly incident on a parabolic layer being perturbed by a plane acoustic wave moving at an angle Ψ with respect to the vertical. This geometry simplifies the problem greatly.

The electron density N is an undisturbed parabolic layer and is described by

$$N = N_{max}\left(\frac{2h}{H} - \frac{h^2}{H^2}\right) , \qquad (17)$$

where H is the layer half-thickness and h is measured from h_o (Fig. 12). The presence of a pressure wave in the ionosphere changes the electron density by an amount [Ref. 6]

$$\frac{\Delta N}{N} = \frac{p-p_o}{p_o}\,\frac{\cos^2\phi}{\gamma} ,$$

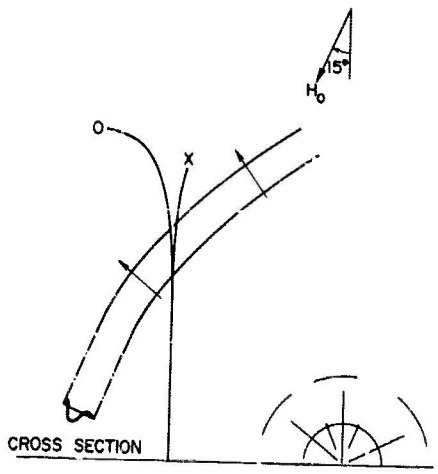

34274

a. Actual situation

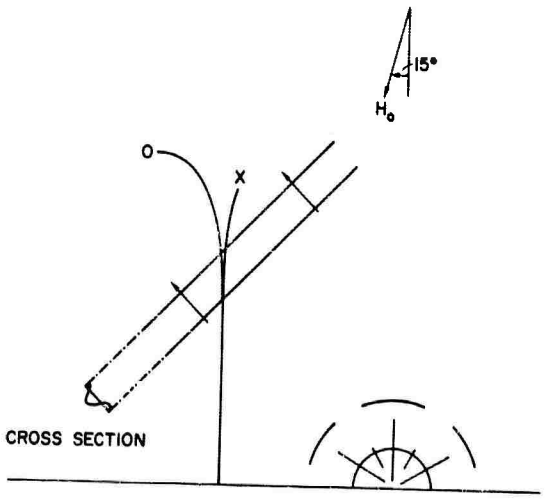

34275

b. Approximation used in calculations

FIG. 11. ACTUAL AND APPROXIMATED ACOUSTIC- AND RADIO-WAVE CONDITIONS FOR VERTICAL-INCIDENCE REFLECTION.

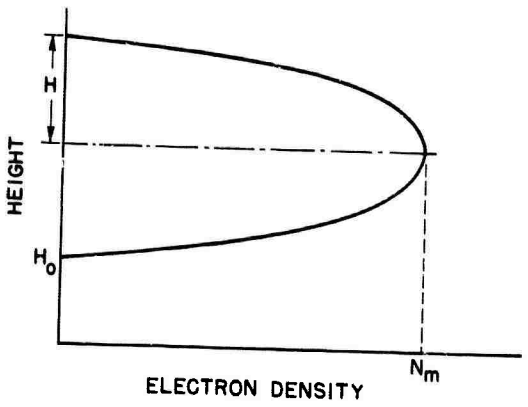

31560

FIG. 12. ELECTRON-DENSITY CURVE FOR PARABOLIC IONOSPHERE.

where Φ is the angle between the magnetic-field lines and the direction of acoustic-wave travel The resulting new density profile is

$$N' = N + \Delta N$$

$$= N_m \left(\frac{2h}{H} - \frac{h^2}{H^2}\right)\left[1 + \left(\frac{p-p_o}{p_o}\frac{\cos^2 \Phi}{\gamma}\right)\right] . \qquad (18)$$

The phase path of a vertically reflected radio wave is found from the integrated index of refraction

$$h' = \int_0^{h_1} \mu \, dh . \qquad (19)$$

For longitudinal propagation of the extraordinary component, the index of refraction μ is given by [Ref. 5]

$$\mu^2 = 1 - \frac{X}{1-|Y_L|} , \qquad (20)$$

where

$$X = \frac{f_{N'}^2}{f^2} = \frac{f_{N_{max}}^2}{f^2}\frac{N'}{N_{max}}$$

and

$$Y_L = \frac{f_H \cos \theta}{f} ,$$

in which $f_{N_{max}}$ = maximum plasma frequency

f_H = gyro frequency

θ = angle between magnetic field and hf path

f = radio frequency.

Substituting the density profile of Eq. (18) into Eq. (19) yields the expression for phase path

$$h' = \int_0^{h_1} \left[\frac{h^2}{CH^2} - \frac{2h}{CH} + 1 \right]^{-1/2} dh \qquad (21)$$

where

$$C = \frac{f(f - f_H \cos\theta)}{f_{N_m}^2 \left\{ 1 + [(p-p_o)/p_o][\cos^2 \phi/\gamma] \right\}} . \qquad (22)$$

The upper limit h_1 of Eq. (21) is the true reflection height and is found by setting the index of refraction to zero--i.e., $X = 1-|Y_L|$. Or, substituting for X and Y_L, one obtains

$$h_1 = H[1 - (1-C)^{1/2}] . \qquad (23)$$

Since the value of C is known as a function of time for a given radio-signal blast-site geometry (Fig. 11), the radio-wave phase path, as a function of time, may be found by substituting Eq. (23) into Eq. (21). The total phase path β, in cycles, is then

$$\beta = \frac{h'f}{c} , \qquad (24)$$

where c is the speed of light and f is the radio-signal frequency.

Equations (21) through (24) allow one to compute β as a function of time for the given neutral atmospheric pressure wave (Fig. 9). Because of the rather complex relationships among these equations, the computations are best done with the aid of a digital computer. The approximations involved are the assumptions of 1) parabolic ionospheric density, 2) an undeflected, extraordinary ray, and 3) a pressure disturbance whose physical size is much larger than the region in which the index of refraction differs appreciably from unity--i.e., much larger than the pressure-sensitive portion of the radio path. The equations were used to calculate the theoretical phase-path and radio-frequency disturbance measured at Arneson and Bow Island during the Snowball test. The results of these calculations are given in Chapter VI of this paper.

III. EXPERIMENTAL EQUIPMENT

The ionosphere above the Snowball explosion was instrumented with four vertical-incidence sounders. Two sounders were located near Arneson, Alberta, 85 km magnetic north of the Suffield Experimental Station; the remaining two were installed at Bow Island, Alberta, 85 km magnetic south of the blast (Fig. 1).

To obtain the greatest possible sensitivity to disturbances in the F region of the ionosphere, the pulse transmitters were operated in the region above the F-layer ordinary-wave critical frequency. These frequencies were measured about 15 min before the blast, and frequencies selected at that time were used throughout the test.

Each sounder operated with a peak-pulse power of about 1 kw. The pulsewidth was 200 μsec, and a 60-pps repetition rate was used. Signals were transmitted and received on separate, horizontal, three-wire, broadband, dipole antennas, whose centers were about 25 ft above ground level. Figure 13 shows a plan view of the transmitting- and receiving-antenna array used at both Bow Island and Arneson.

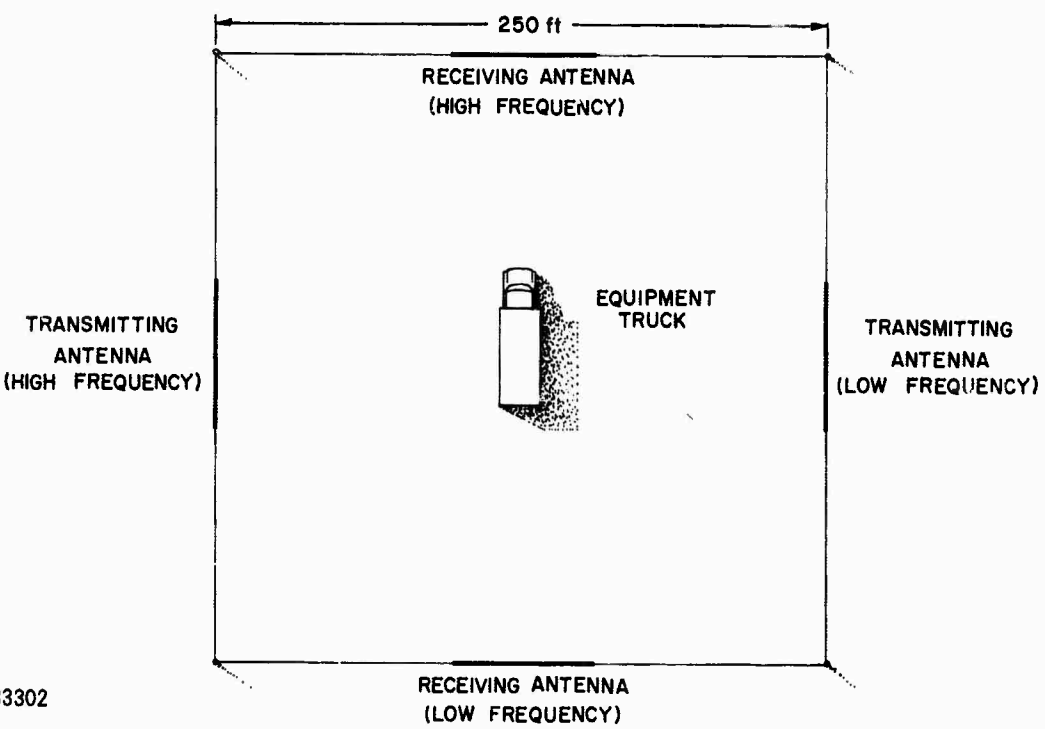

FIG. 13. PLAN VIEW OF TRANSMITTING AND RECEIVING ANTENNA ARRAY USED AT BOW ISLAND AND ARNESON.

The output of each receiver was translated down to 25 kc and recorded on one channel of a Sanborn Model 2007, seven-channel magnetic tape recorder employing standard direct-record electronics. WWV signals were simultaneously recorded on an adjacent channel for timing purposes. A block diagram of the system is shown in Fig. 14.

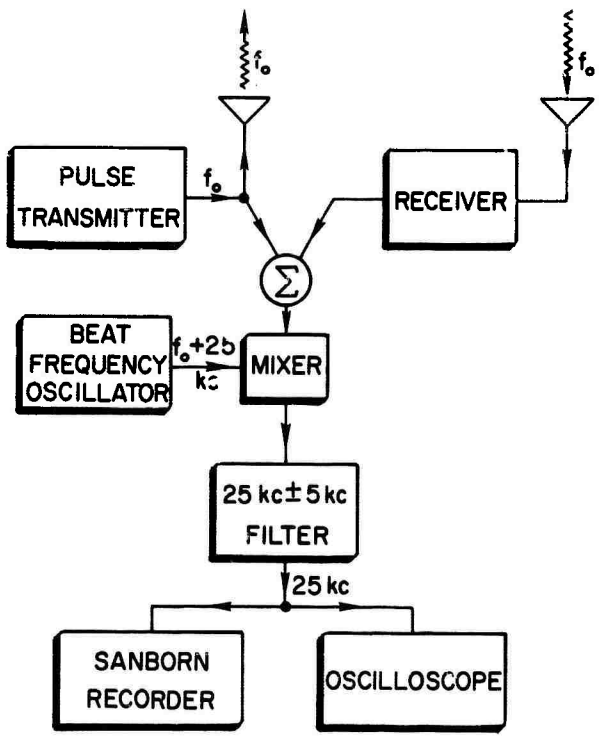

34276

FIG. 14. BLOCK DIAGRAM OF A TRANSMITTER-RECEIVER PAIR (two at each site).

Figure 15 shows a typical signal recorded in this manner for a single transmitted pulse. The 200-μsec burst of 25-kc signal derived from the transmitter rf pulse is followed by about 2 msec of delay corresponding to the earth-ionosphere-earth travel time.

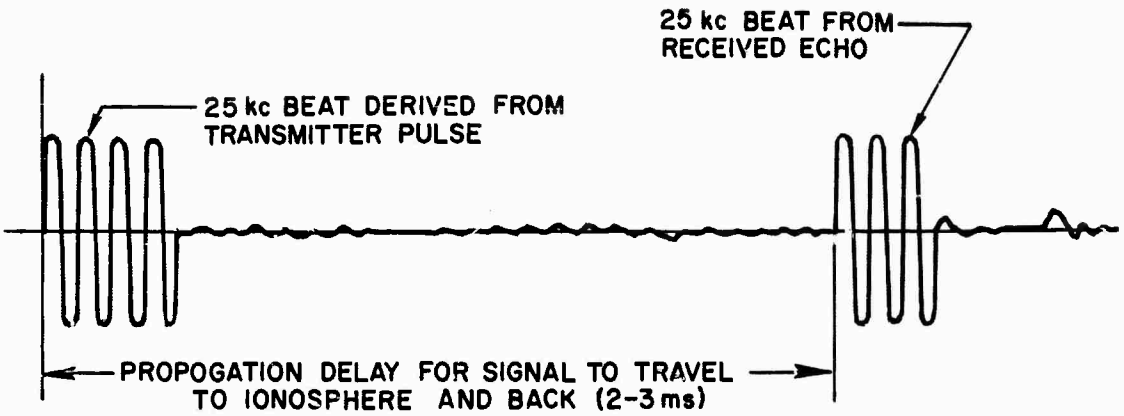

34277

FIG. 15. A TYPICAL RECEIVER OUTPUT SIGNAL.

Previous page was blank, therefore not filmed.

IV. DATA PROCESSING

The data taken at Bow Island and Arneson were recorded on magnetic tape continuously from 90 min before detonation until 45 min afterward. Figure 15 shows the recorded signal as displayed on an oscilloscope for one typical transmitted pulse and received echo. The magnetic tapes recorded on-site were later processed at Stanford to produce range-time film records showing received signal phase.

The film records were generated in the following manner. An oscilloscope sweep was triggered using the leading edge of the 25-kc signal derived from the transmitted radio-frequency pulse. The sweep was then intensity modulated with the remaining recorded waveform. The result was a line across the face of the oscilloscope containing a series of dots corresponding to the peaks of the signal shown in Fig. 15. By moving a 35-mm film strip perpendicular to the sweep, the dots from each successive oscilloscope trace were recorded on a slightly different portion of the film. The film was moved slowly enough to allow a series of pulses recorded in this manner to appear as lines or "stripes" on the film strip.

Figure 16 shows a typical "stripe" recording taken from a normal, undisturbed ionosphere. The transmitted pulses may be seen at the bottom of the recording as several parallel lines. The received pulses appear higher up on the record as diagonal lines. A measure of the phase change introduced by ionospheric fluctuations may be obtained by counting the number of stripes that cross a given horizontal line through the received pulses. Since each stripe represents a 2π-radian phase change, the relative phase in the path, as a function of time, may be plotted directly from these records. The change in frequency of the received radio wave is then simply the derivative of the phase-time record.

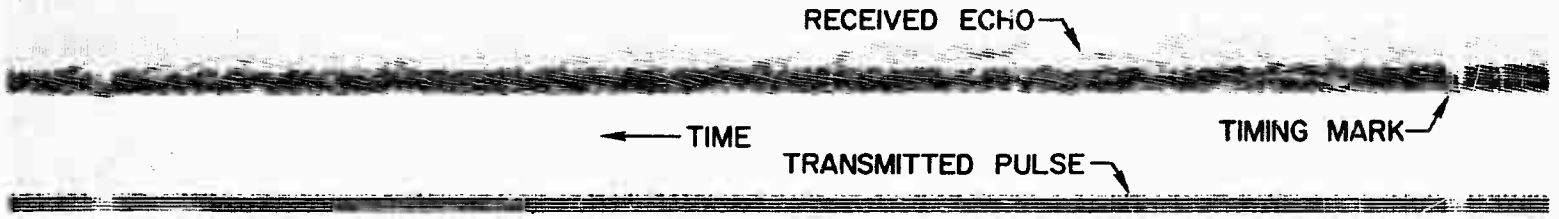

FIG. 16. TYPICAL STRIPE RECORDING TAKEN DURING NORMAL, UNDISTURBED PERIOD.

V. RESULTS

At the time of the Snowball test, which occurred at 10:58 MST on 17 July, 1964, all four pulse sounders were operating satisfactorily. The two Arneson transmitters were placed on 5.6 Mc and 5.7 Mc while those at Bow Island operated on 5.2 Mc and 4.5 Mc. These frequencies were chosen on the basis of the measured 5.4-Mc ordinary-wave critical frequency in the hope that the return echoes would contain extraordinary-wave components only (see Chapter II).

Clear, explosion-induced disturbances were detected about 9½ min after detonation on all frequencies except 5.2 Mc. Because this frequency was well below the critical frequency, both ordinary and extraordinary waves were reflected from the ionosphere with little attenuation. As a result, the return echoes from successive transmitted pulses overlapped and produced a film-strip record in which the F-layer perturbation was indiscernable.

The clearest effect was measured at the 5.4-Mc Bow Island site. Figure 17 shows the "stripe" records taken immediately before and during the ionospheric disturbance on this frequency. The effect is characterized by a sudden change in the slope of the return echoes and is most noticeable at about 10 min after detonation. A mixing of extraordinary-wave (lower return echo) and ordinary-wave (upper return echo) signals occurs at about 10 min 30 sec. Similar disturbances were measured at the Arneson site. No ordinary components appeared on 5.6 and 5.7 Mc, however, because the transmitters were operating about 200 kc above O-wave critical.

The phase-vs-time record taken from the 5.4-Mc Bow Island "stripe" recording is shown in Fig. 18. A measure of the effect due to the explosion was obtained by drawing on the phase plot a curve which was considered to be a best approximation to the undisturbed ionospheric return. The difference between the two curves then gave the phase disturbance vs time record. All records were reduced in the above manner. The results are summarized in Fig. 19.

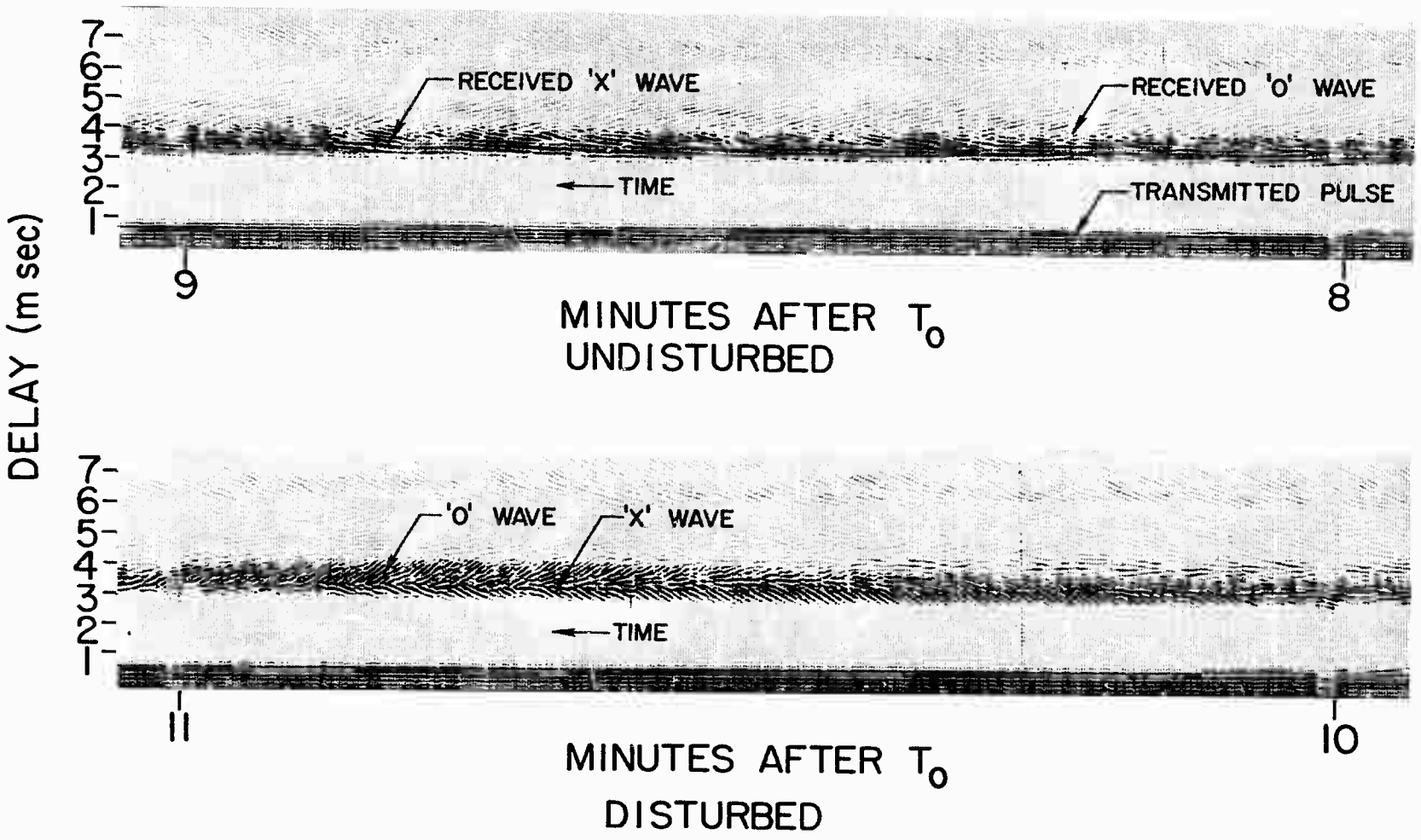

FIG. 17. STRIPE RECORDING TAKEN AT BOW ISLAND DURING DISTURBED PERIOD.

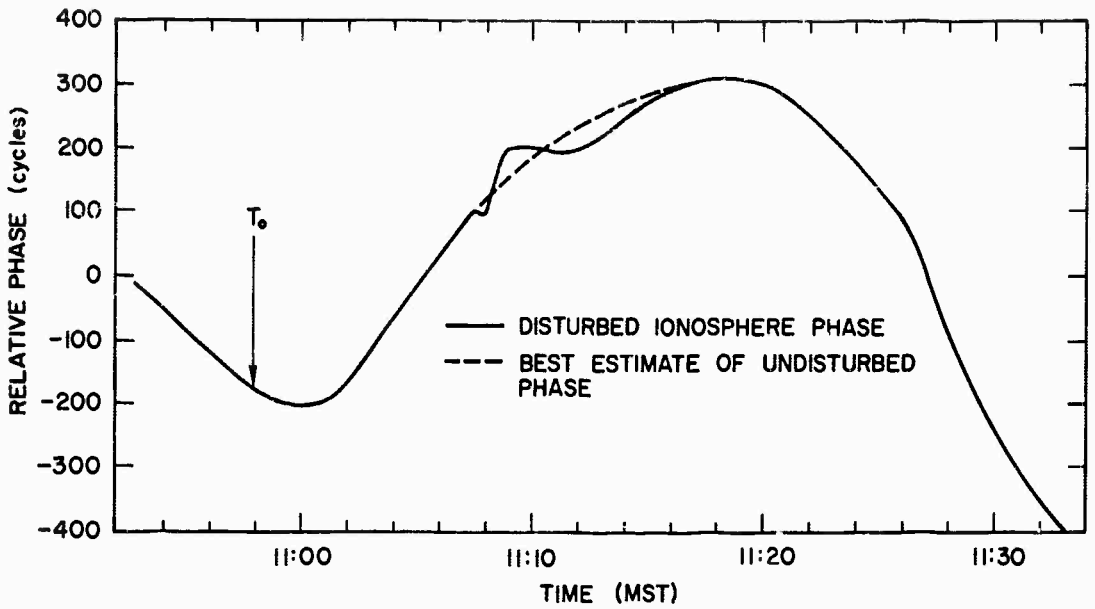

34278

FIG. 18. PHASE VS TIME TAKEN FROM BOW ISLAND 5.4-MC STRIPE RECORDING.

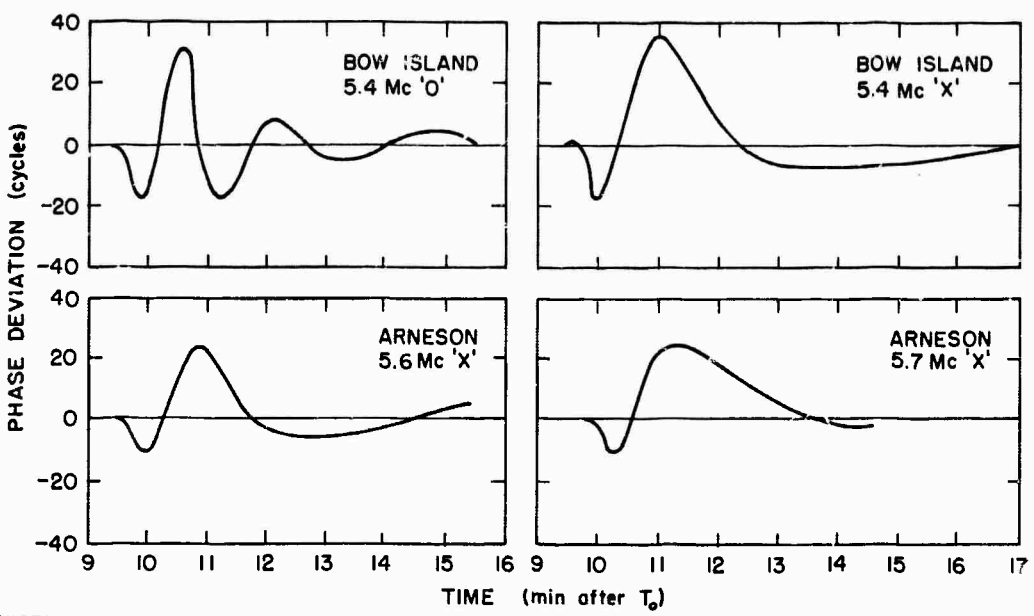

34279

FIG. 19. PHASE-DISTURBANCE RECORDS MEASURED AT BOW ISLAND AND ARNESON AFTER DETONATION.

VI. COMPARISON OF THEORETICAL AND EXPERIMENTAL RESULTS

The purpose of the following section is to compare the experimental results summarized in Chapter V with curves based on the linear acoustic theory presented in Chapter II. Two sets of on-site data--the atmospheric-wind profile and the ionospheric-electron-density profile--were used in calculating the theoretical waveforms.

The estimated horizontal component of wind blowing in the Bow Island-Arneson direction during the explosion is shown in Fig. 20. Data for this curve were compiled from several sources. The 0-to-20-km winds, for example, were measured with a weather balloon released at the test

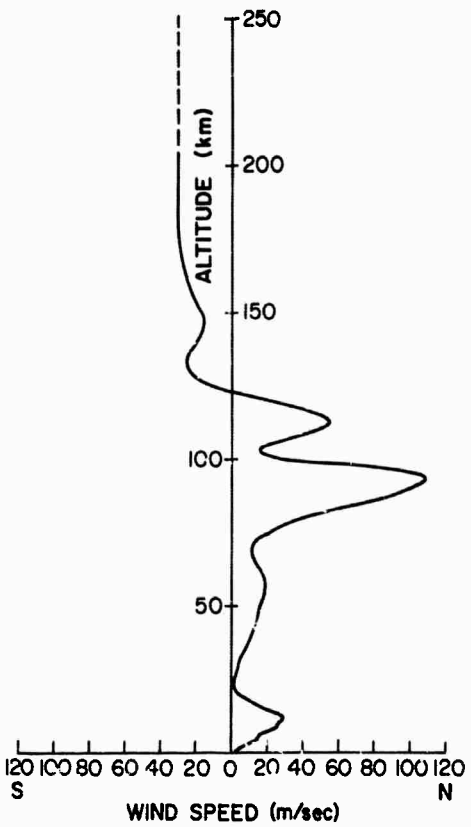

34280

FIG. 20. ESTIMATED WIND PROFILE OVER SUFFIELD AT TIME OF BLAST.

site shortly before T_o. Sounding rockets fired at Cold Lake, Alberta (about 300 miles north of Suffield), about one hour after the blast provided data to an altitude of 80 km. No measurements above this height, however, were taken during the test; the results above 80 km shown in Fig. 20 were estimated on the basis of a survey of several articles giving data on high-altitude winds [Refs. 7-10].

The nearest measured electron-density profile at the time of the test was taken at Kenora, near Winnipeg, Manitoba, with an NBS C-4 sounder. Figure 21 shows the ionogram from this station. The ordinary-wave critical frequency is seen to be about 5.0 Mc. To obtain the best estimate of electron density above the blast site at Suffield, Alberta, this record was scaled upward in frequency so that the critical frequency corresponded to the 5.4-Mc critical frequency measured with the Stanford sounders at Bow Island and Arneson (Chapter V).

Radio-wave and acoustic raytracings (Figs. 22 and 23) based on the experimental wind and electron-density profiles outlined above were generated using digital raytracing capabilities available at Stanford Electronics Laboratories. These curves were superimposed to obtain the onset time of the disturbance--the time at which the acoustic wave reaches the radio-wave reflection point--and the angles Φ (the angle between magnetic field lines and direction of acoustic-wave propagation) and Ψ (the angle between the acoustic-ray direction and the vertical).

The theoretical radio-wave frequency disturbances were then calculated with the appropriate values of Φ and Ψ above and the methods given in Chapter II, Section B. A comparison between the waveforms obtained in this manner and the experimental results is shown in Fig. 24. Table 1 shows the onset-time comparison.

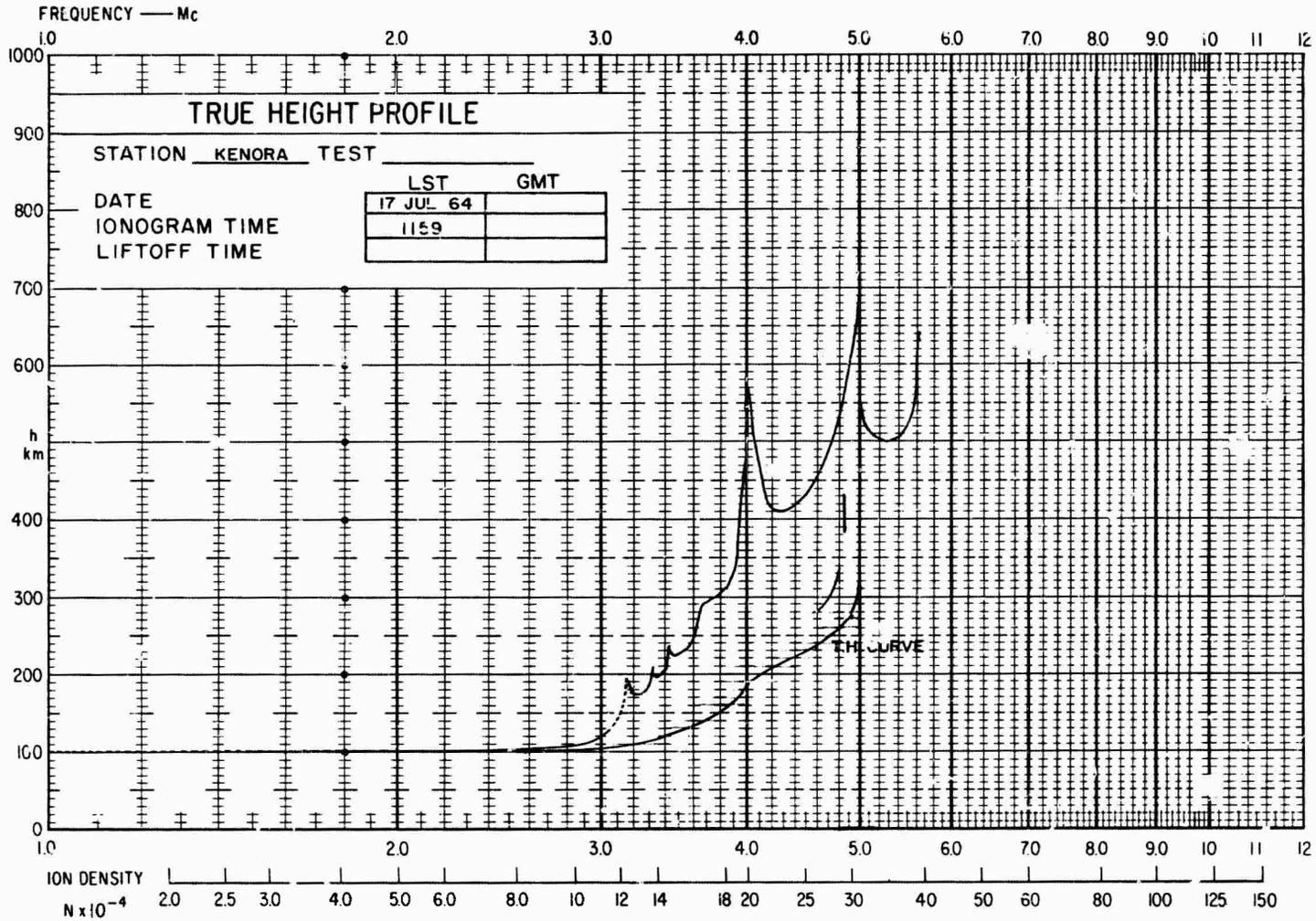

FIG. 21. VERTICAL-INCIDENCE IONOGRAM TAKEN AT KENORA, MANITOBA.

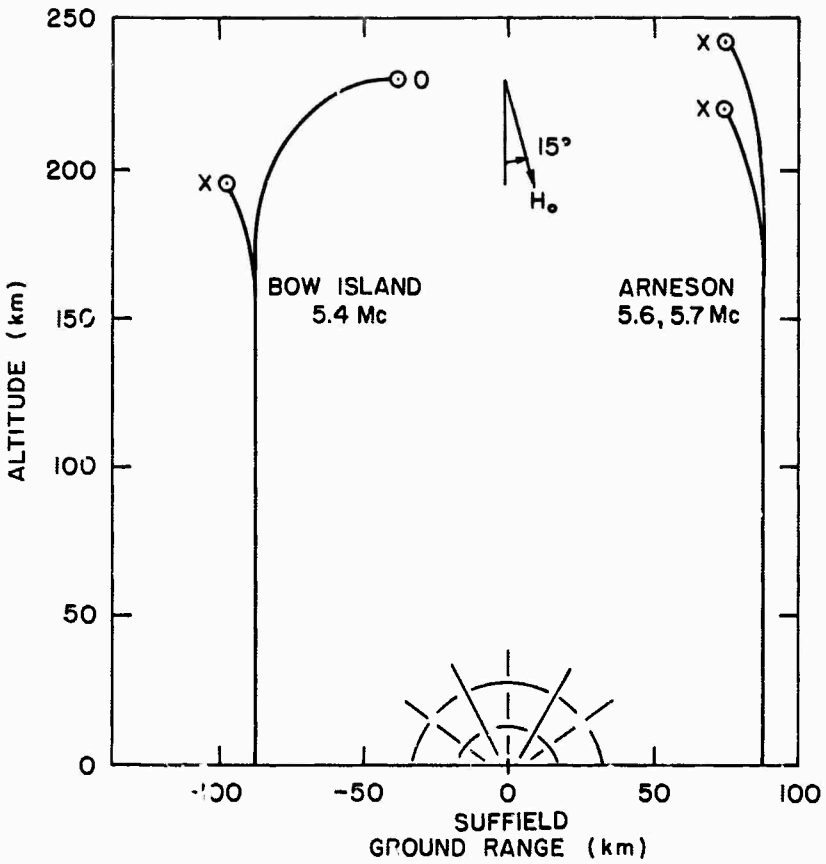

FIG. 22. RADIO-WAVE RAYTRACING BASED ON EXPERIMENTAL ELECTRON-DENSITY PROFILE.

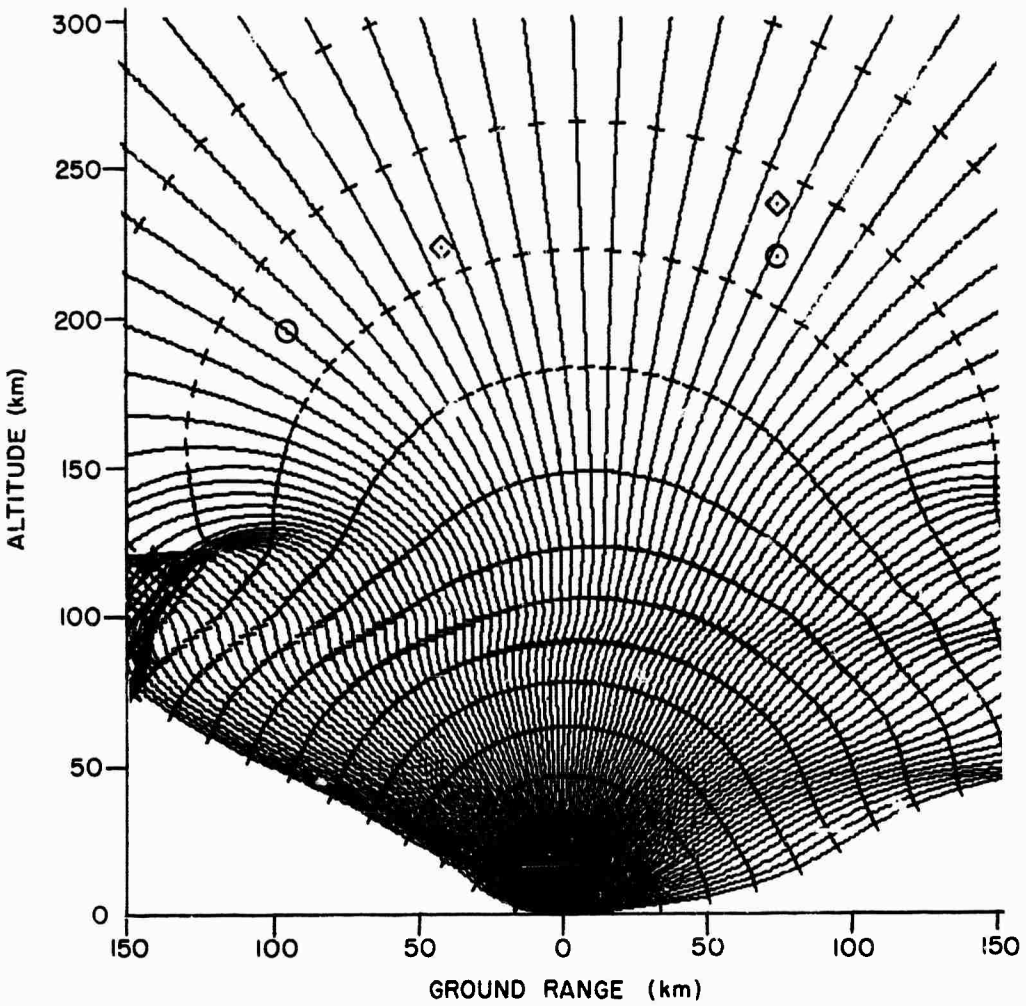

FIG. 23. ACOUSTIC RAYTRACING OVER SUFFIELD BASED ON EXPERIMENTAL WIND PROFILE.

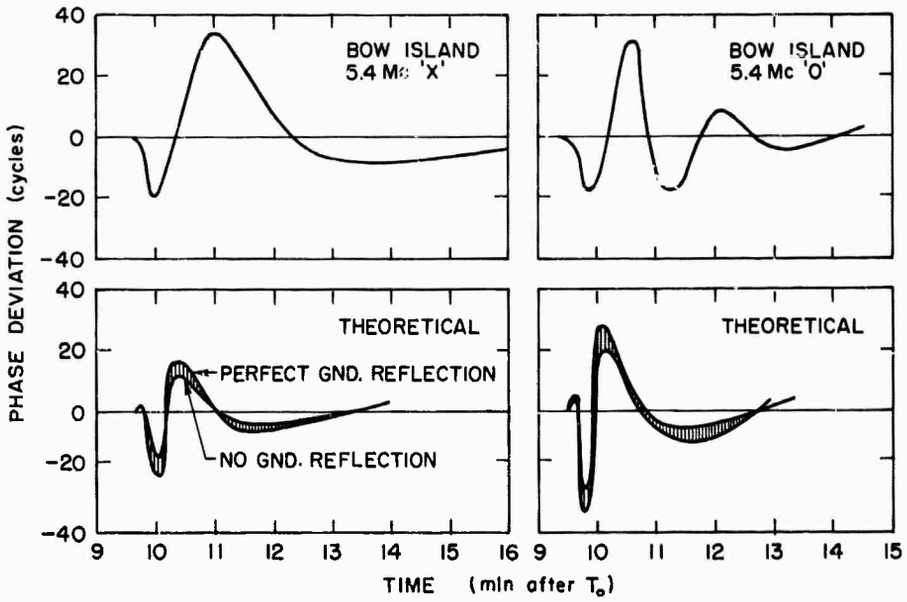

34282

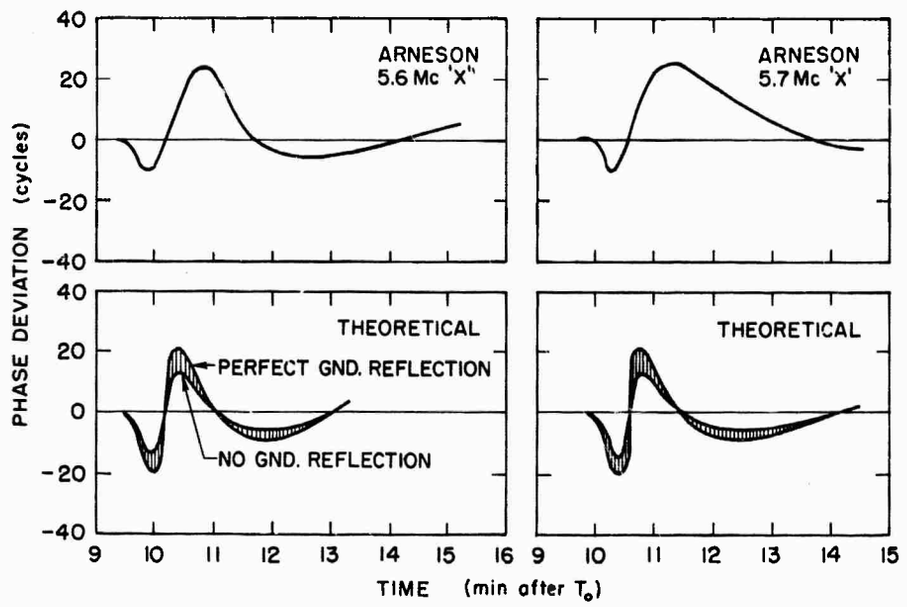

34283

FIG. 24. COMPARISON OF EXPERIMENTAL AND THEORETICAL PHASE-DISTURBANCE RECORDS.

TABLE 1. COMPARISON OF DISTURBANCE ONSET TIMES

Field Site	Frequency (Mc)	Wave	Experimental Onset Time (Min)	Theoretical Onset Time (Min)
Bow Island	5.4	O	+ 9.4	+ 9.5
Bow Island	5.4	X	+ 9.6	+ 9.7
Arneson	5.6	X	+ 9.5	+ 9.5
Arneson	5.7	X	+ 9.9	+ 9.8

Previous page was blank, therefore not filmed.

VII. CONCLUSIONS

The experiment described in this paper has demonstrated the effectiveness of using a relatively simple linear acoustic theory to describe the propagation of explosion-induced disturbances to large distances. Figure 24 and Table 1 summarize the comparison between results obtained experimentally and those calculated with the linear model. The agreement is quite good, particularly in Table 1--the disturbance-onset-time results. Inspection of Fig. 24 shows that the period of the predicted disturbance is slightly shorter than that measured experimentally, but the wave shape and the amplitude of the predicted phase disturbance compare well with the experimental results.

This comparison strengthens the confidence in the sound-velocity profile used in the model and suggests that the assumed atmospheric-filter characteristics (Fig. 7) may be in error--that is, the real atmosphere appears to have a smaller bandpass region than shown in Fig. 7. Since the shape of the filter is a critical function of the atmospheric conditions near the radio-wave reflection point, it may be possible to obtain some information about high-altitude constituents by "fitting" a filter to match the observed waveform.

No definitive conclusion about the effect of the earth's magnetic field on acoustic-wave propagation can be drawn from the results of this experiment. It was stated in Chapter II that the degree to which a neutral acoustic wave produces a corresponding charged-particle disturbance is proportional to $\cos^2 \phi$ (ϕ is the angle between the acoustic-wave direction and the magnetic field). In an attempt to verify this dependence, sounders were placed 85 km magnetic north and south of the blast. Prior to the experiment, it was expected that this geometrical arrangement would provide a ϕ of about 30 deg over the south site and 60 deg at the north site. Thus, a three-to-one ratio in measured amplitude was expected.

Unfavorable northerly winds at the time of the blast (Fig. 20), however, changed these angles to about 37 deg and 41 deg respectively. This change is equivalent to a 1.1/1 amplitude ratio and is well within experimental error.

REFERENCES

1. H. L. Brode, "Blast Wave from a Spherical Charge," Phys. of Fluids, 2, Mar-Apr 1959, pp. 217-229.

2. J.W.S. Rayleigh, The Theory of Sound, Dover Publications, New York, 1945.

3. U. S. Standard Atmosphere, NASA, U. S. Air Force, U. S. Weather Bureau, 1962.

4. H. H. Skilling, Electric Transmission Lines, McGraw-Hill Book Co., Inc., New York, 1951, pp. 353-354.

5. J. A. Ratcliffe, The Magneto-Ionic Theory and Its Applications to the Ionosphere, Cambridge University Press, Cambridge, England, 1959.

6. Lowell Holway, Jr., D. Kahn, and E. Rolfe, "Investigation of Traveling Waves in the Ionosphere and Their Effects," Final Report, Contract No. AF19(628)-2802, Dec 1963, pp. 12-14.

7. E. Manning et al, "Some Wind Determinations in the Upper Atmosphere Using Artificially Generated Sodium Clouds," J. Geophys. Res., 64, 6, Jun 1959, pp. 587-591.

8. W. G. Stroud, W. Nordberg, and J. R. Walsh, "Atmospheric Temperatures and Winds Between 30 and 80 Km," J. Geophys. Res., 61, 1, Mar 1956, pp. 45-46.

9. W. G. Stroud et al., "Rocket Grenade Measurements of Temperatures and Winds in the Ionosphere over Churchill, Canada," J. Geophys. Res., 65, 8, Aug 1960, pp. 2307-2323.

10. J. W. Findlay, "Moving Clouds of Ionization in Region E of the Ionosphere," J. Atmos. Terrest. Phys., 3, 2, 1952, pp. 73-78.

UNCLASSIFIED
Security Classification

DOCUMENT CONTROL DATA - R&D

(Security classification of title, body of abstract and indexing annotation must be entered when the overall report is classified)

1. ORIGINATING ACTIVITY (Corporate author)
Stanford Electronics Laboratories
Stanford University, Stanford, California

2a. REPORT SECURITY CLASSIFICATION
UNCLASSIFIED

2b. GROUP

3. REPORT TITLE
HF RADIO MEASUREMENTS OF THE HIGH-ALTITUDE ACOUSTIC EFFECTS OF A GROUND-LEVEL EXPLOSION

4. DESCRIPTIVE NOTES (Type of report and inclusive dates)
Technical Report

5. AUTHOR(S) (Last name, first name, initial)
L. J. Griffiths, G. H. Barry and J. C. Taenzer

6. REPORT DATE	7a. TOTAL NO. OF PAGES	7b. NO. OF REFS
May 1965	36	10

8a. CONTRACT OR GRANT NO.	9a. ORIGINATOR'S REPORT NUMBER(S)
ONR Contract Nonr-225(64)	SU-SEL-65-062
b. PROJECT NO. and ARPA Order 196-65	Technical Report No. 107
c.	9b. OTHER REPORT NO(S) (Any other numbers that may be assigned this report)
d.	

10. AVAILABILITY/LIMITATION NOTICES
Foreign announcement and dissemination by DDC not authorized.

11. SUPPLEMENTARY NOTES	12. SPONSORING MILITARY ACTIVITY

13. ABSTRACT

An hf radio experiment was performed to measure the high-altitude effect of the vertically traveling pressure wave resulting from a large ground-level explosion. The blast--Project Snowball--consisted of 500 tons of TNT and was detonated at the Suffield Experimental Station, Alberta, Canada, July, 1964. The ionospheric disturbance was monitored using vertical-incidence, phase-sensitive sounders located 85 km from ground zero.

Simple, linear, acoustic theory was used to calculate the onset time, amplitude, and period of the radio-signal disturbance. These calculations agree closely with measurements taken by the vertical-incidence sounders--onset time was predicted within 10 sec, and both amplitude and period agreed within a factor of two.

DD FORM 1 JAN 64 1473

UNCLASSIFIED
Security Classification

14. KEY WORDS	LINK A		LINK B		LINK C	
	ROLE	WT	ROLE	WT	ROLE	WT
ACOUSTICS EXPLOSION EFFECTS IONOSPHERIC DISTURBANCES						

INSTRUCTIONS

1. ORIGINATING ACTIVITY: Enter the name and address of the contractor, subcontractor, grantee, Department of Defense activity or other organization *(corporate author)* issuing the report.

2*a*. REPORT SECURITY CLASSIFICATION: Enter the overall security classification of the report. Indicate whether "Restricted Data" is included. Marking is to be in accordance with appropriate security regulations.

2*b*. GROUP: Automatic downgrading is specified in DoD Directive 5200.10 and Armed Forces Industrial Manual. Enter the group number. Also, when applicable, show that optional markings have been used for Group 3 and Group 4 as authorized.

3. REPORT TITLE: Enter the complete report title in all capital letters. Titles in all cases should be unclassified. If a meaningful title cannot be selected without classification, show title classification in all capitals in parenthesis immediately following the title.

4. DESCRIPTIVE NOTES: If appropriate, enter the type of report, e.g., interim, progress, summary, annual, or final. Give the inclusive dates when a specific reporting period is covered.

5. AUTHOR(S): Enter the name(s) of author(s) as shown on or in the report. Enter last name, first name, middle initial. If military, show rank and branch of service. The name of the principal author is an absolute minimum requirement.

6. REPORT DATE: Enter the date of the report as day, month, year, or month, year. If more than one date appears on the report, use date of publication.

7*a*. TOTAL NUMBER OF PAGES: The total page count should follow normal pagination procedures, i.e., enter the number of pages containing information.

7*b*. NUMBER OF REFERENCES: Enter the total number of references cited in the report.

8*a*. CONTRACT OR GRANT NUMBER: If appropriate, enter the applicable number of the contract or grant under which the report was written.

8*b*, 8*c*, & 8*d*. PROJECT NUMBER: Enter the appropriate military department identification, such as project number, subproject number, system numbers, task number, etc.

9*a*. ORIGINATOR'S REPORT NUMBER(S): Enter the official report number by which the document will be identified and controlled by the originating activity. This number must be unique to this report.

9*b*. OTHER REPORT NUMBER(S): If the report has been assigned any other report numbers *(either by the originator or by the sponsor)*, also enter this number(s).

10. AVAILABILITY/LIMITATION NOTICES: Enter any limitations on further dissemination of the report, other than those imposed by security classification, using standard statements such as:

(1) "Qualified requesters may obtain copies of this report from DDC."

(2) "Foreign announcement and dissemination of this report by DDC is not authorized."

(3) "U. S. Government agencies may obtain copies of this report directly from DDC. Other qualified DDC users shall request through _____."

(4) "U. S. military agencies may obtain copies of this report directly from DDC. Other qualified users shall request through _____."

(5) "All distribution of this report is controlled. Qualified DDC users shall request through _____."

If the report has been furnished to the Office of Technical Services, Department of Commerce, for sale to the public, indicate this fact and enter the price, if known.

11. SUPPLEMENTARY NOTES: Use for additional explanatory notes.

12. SPONSORING MILITARY ACTIVITY: Enter the name of the departmental project office or laboratory sponsoring *(paying for)* the research and development. Include address.

13. ABSTRACT: Enter an abstract giving a brief and factual summary of the document indicative of the report, even though it may also appear elsewhere in the body of the technical report. If additional space is required, a continuation sheet shall be attached.

It is highly desirable that the abstract of classified reports be unclassified. Each paragraph of the abstract shall end with an indication of the military security classification of the information in the paragraph, represented as *(TS)*, *(S)*, *(C)*, *or (U)*.

There is no limitation on the length of the abstract. However, the suggested length is from 150 to 225 words.

14. KEY WORDS: Key words are technically meaningful terms or short phrases that characterize a report and may be used as index entries for cataloging the report. Key words must be selected so that no security classification is required. Identifiers, such as equipment model designation, trade name, military project code name, geographic location, may be used as key words but will be followed by an indication of technical context. The assignment of links, roles, and weights is optional.